January 24, 2008 18:7 WSPC/130-JCA 00339

INTERNATIONAL ASSOCIATION
FOR MATHEMATICS AND
COMPUTERS IN SIMULATION

3

NULL-FIELD INTEGRAL EQUATION APPROACH FOR EIGENPROBLEMS WITH CIRCULAR BOUNDARIES

5

J. T. CHEN*

7

*Department of Harbor and River
National Taiwan Ocean University
2 Pei-Ning Road Keelung Taiwan 202-24, R.O.C
jtchen@mail.ntou.edu.tw*

9

C. T. CHEN

11

*CTCI Corporation, 10 Fl., CTCI Tower, 77, Sec. 2
Tun Hwa South Road, Taipei, Taiwan 106, R.O.C.
onion0214@ctci.com.tw*

13

I. L. CHEN

15

*Department of Naval Architecture
National Kaohsiung Marine University
Kaohsiung, Taiwan
ilchen@mail.nkmu.edu.tw*

17

21 In this paper, the eigenproblems with circular boundaries of multiply-connected domain are studied by using the null-field integral equations in conjunction with degenerate kernels and Fourier series to
23 avoid calculating the Cauchy and Hadamard principal values. An adaptive observer system of polar coordinate is considered to fully employ the property of degenerate kernels. For the hypersingular
25 equation, vector decomposition for the radial and tangential gradients is carefully considered in the polar coordinate system. Direct-searching scheme is employed to detect the eigenvalues by using
27 the singular value decomposition (SVD) technique. Both the singular and hypersingular equations result in spurious eigenvalues which are the associated interior Dirichlet and Neumann problems of
29 interior domain of inner circles, respectively. It is analytically verified that the spurious eigenvalue depends on the radius of any inner circle and numerical experiments support this point. Several
31 examples are demonstrated to see the validity of the present formulation. More number of degrees of freedom of BEM is required to obtain the same accuracy of the present approach.

33 *Keywords*: Null-field integral equation; singular value decomposition; degenerate kernel; Fourier series; eigenproblem.

http://ind.ntou.edu.tw/~msvlab/

1. Introduction

During the recent decades, many numerical methods are utilized to solve the engineering problems. The FEM and BEM have been recognized as the effective methods in numerical analysis. Although FEM is a popular method for solving eigenproblems, it needs a lot of time to generate the mesh for problems with complex geometries. In this aspect, BEM is an efficient alternative from the viewpoint of mesh reduction. However, it also exist some pitfalls in BEM and the readers can consult with the keynote lecture by Chen *et al.*[1] for the detailed discussion.

For the Helmholtz problems, it is well known that the boundary integral equation for solving the exterior and interior problems results in fictitious frequency and spurious eigenvalue, respectively. In the interior eigenproblem with a simply-connected domain, the dual reciprocity method (DRM) by Partridge *et al.*[2] and the multiple reciprocity method (MRM)[3-5] have been widely used. One advantage of using the conventional MRM is that only real-valued computation is considered instead of complex-valued computation since the fundamental solution for Laplace operator is used.[6] Nevertheless, no matter what we used either the real-part singular or the hypersingular equation, the spurious eigenvalues occur. To overcome the problem of spurious eigenvalue, the dual MRM by Chen *et al.*[7] the real-part dual BEM by Kuo *et al.*[8] and the singular value decomposition (SVD) updating terms[1,7,8] had been constructed. Chen *et al.*[1,7,9,10] also extended the combined Helmholtz exterior integral equation formulation (CHEEF) concept, Fredholm alternative theorem and SVD updating technique to filter out the spurious eigenvalue. Tai and Shaw[11] claimed that spurious eigenvalues do not appear if a complex-valued kernel is employed. However, it is true only for simply-connected domain. For a multiply-connected problem, the spurious eigensolution also appears even though a complex-valued BEM is employed to solve the eigensolution. Spurious eigenvalues were found by Kitahara[12] and were suppressed by Chen *et al.*[13] Recently, spurious eigensolutions in the BEM[14,15] and method of fundamental solution (MFS)[16,17] have been noticed until the recent years. Some remedies, *e.g.* SVD updating technique and Burton & Miller method were also presented to filter out the spurious eigenvalues.

For the problems with a circular geometry, the Fourier series expansion method is specially suitable to obtain the analytical solution. Lin[18] employed the transformation technique of cylindrical wave functions to satisfy the boundary condition with seven holes. Nagaya and Poltorak[19] used both the Fourier expansion collocation method and point-matching approach to find the eigenvalues with eccentric inner boundaries. Mogilevskaya *et al.*,[20-22] Barone and Caulk,[23-29] Bird and Steele[30,31] attempted to solve problems involving circular boundary using series expansions. Barone and Caulk used the special boundary integral method for solving the Laplace's equation in two-dimensional domains with circular holes. According to their idea, the boundary potential and its normal derivative were expressed in a finite series of circular harmonics on each hole. Unlike other approaches, the unknown coefficients in each hole are determined by a new set of integral equations with special kernel functions. However, the explicit equations[29] were limited to the case when a constant

potential is specified on the boundary of each hole. For the eigenproblem with circular boundaries, Chen *et al.*[14] have employed BEM to demonstrate the existence of spurious eigenvalues. Also, they proposed several regularization techniques to filter out the spurious solution. However, low frequency behavior was not well described. This motivates us to consider BIEM using Fourier expansion to more analytically solve the problem with circular boundaries.

In this paper, the boundary integral equation method (BIEM) is utilized to solve the eigenproblems with circular boundaries. To fully utilize the geometry of circular boundary, not only Fourier series for boundary densities as used by many researchers but also the degenerate kernel for fundamental solutions in the present formulation are incorporated into the null-field integral equation at the same time. All the boundary integrals are analytically determined by using the orthogonal property of the Fourier bases. The principal values of improper integrals are replaced by the series sum. In integrating each circular boundary for the null-field equation, the observer system of polar coordinate is adaptively considered to fully employ the property of degenerate kernel. For the hypersingular equation, vector decomposition for the radial and tangential gradients is carefully considered, especially in case of eccentric case. Direct-searching scheme is employed to detect the eigenvalue by using the SVD technique. Spurious eigenvalues in the multiply-connected problems are also examined. Mode shapes are simultaneously determined from the right unitary vectors of zero singular value in the SVD after we detect the zero singular value in case of eigenvalue. The results are compared with those of FEM and BEM.

2. Problem Statement and Integral Formulation

2.1. *Problem statement*

The governing equation of the acoustic problem is the Helmholtz equation

$$(\nabla^2 + k^2)u(x) = 0, \quad x \in D^I \tag{1}$$

where ∇^2, k and D are the Laplacian operator, the wave number, and the domain of interest, respectively. Consider the eigenproblem with a circular domain containing N_c randomly distributed circular holes centered at the position vector $\underset{\sim}{c_j}$ $(j = 1, 2, \ldots, N_c)$ as shown in Fig. 1.

2.2. *Dual boundary integral formulation*

Based on the dual boundary integral formulation of the domain point for the eigenproblem,[13] we have

$$2\pi u(x) = \int_B T(s, x)u(s)dB(s) - \int_B U(s, x)t(s)dB(s), \quad x \in D^I \tag{2}$$

$$2\pi t(x) = \int_B M(s, x)u(s)dB(s) - \int_B L(s, x)t(s)dB(s), \quad x \in D^I \tag{3}$$

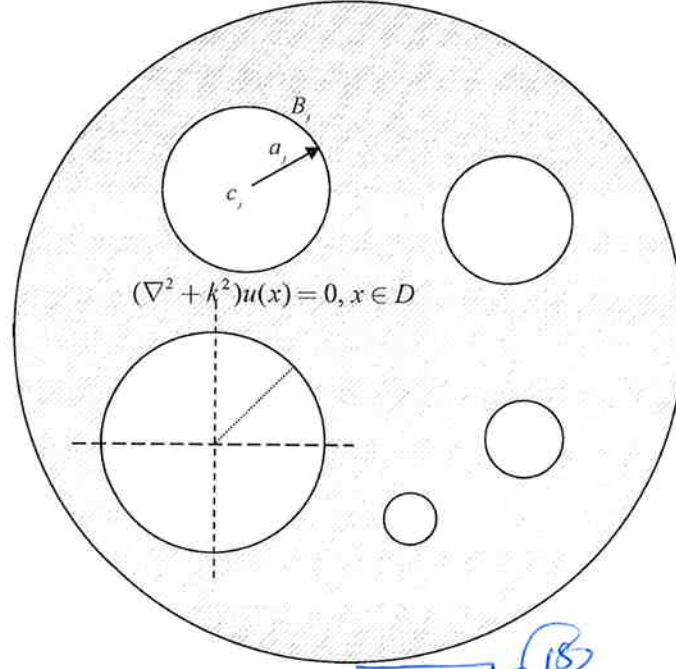4   *J. T. Chen, C. T. Chen & I. L. Chen*

Fig. 1. Problem statement.

where s and x are the source and field points, respectively, D^I is the domain of the interests, $t(s)$ is the directional derivative of $u(s)$ along the outer normal direction at s. The $U(s, x)$, $T(s, x)$, $L(s, x)$ and $M(s, x)$ represent the four kernel functions[13]

$$U(s, x) = \frac{-i\pi H_0^{(1)}(kr)}{2},$$ (4)

$$T(s, x) = \frac{\partial U(s, x)}{\partial n_s} = \frac{-ik\pi H_1^{(1)}(kr)}{2} \frac{y_i n_i}{r},$$ (5)

$$L(s, x) = \frac{\partial U(s, x)}{\partial n_x} = \frac{ik\pi H_1^{(1)}(kr)}{2} \frac{y_i \bar{n}_i}{r},$$ (6)

$$M(s, x) = \frac{\partial^2 U(s, x)}{\partial n_x \partial n_s} = \frac{-ik\pi}{2} \left[-k \frac{H_2^{(1)}(kr)}{r^2} y_i y_j n_i \bar{n}_j + \frac{H_1^{(1)}}{r} n_i \bar{n}_i \right],$$ (7)

where $H_n^{(1)}(kr)$ is the nth order Hankel function of the first kind, $r = |x - s|$, $y_i = s_i - x_i$, $i^2 = -1$, n_i and $\bar{n}_i$ are the ith components of the outer normal vectors at s and x, respectively. Equations (2) and (3) are referred to singular and hypersingular boundary integral equation (BIE), respectively.

1   ### 2.3. *Null-field integral formulation in conjunction the degenerate kernel and Fourier series*

By collocating x outside the domain ($x \in D^E$), we obtain the null-field integral equations as shown below[13]:

$$0 = \int_B T(s,x)u(s)dB(s) - \int_B U(s,x)t(s)dB(s), \quad x \in D^E, \tag{8}$$

$$0 = \int_B M(s,x)u(s)dB(s) - \int_B L(s,x)t(s)dB(s), \quad x \in D^E. \tag{9}$$

By using the polar coordinate, we can express $x = (\rho, \phi)$ and $s = (R, \theta)$. The four kernels, U, T, L and M can be expressed in terms of degenerate kernels as shown below[13]:

$$U(s,x) = \begin{cases} U^I(s,x) = \dfrac{-\pi i}{2} \displaystyle\sum_{m=-\infty}^{\infty} J_m(k\rho)H_m^{(1)}(kR)\cos(m(\theta-\phi)), & R \geq \rho \\[2em] U^E(s,x) = \dfrac{-\pi i}{2} \displaystyle\sum_{m=-\infty}^{\infty} H_m^{(1)}(k\rho)J_m(kR)\cos(m(\theta-\phi)), & \rho > R \end{cases}, \tag{10}$$

$$T(s,x) = \begin{cases} T^I(s,x) = \dfrac{-\pi k i}{2} \displaystyle\sum_{m=-\infty}^{\infty} J_m(k\rho)H_m'^{(1)}(kR)\cos(m(\theta-\phi)), & R > \rho \\[2em] T^E(s,x) = \dfrac{-\pi k i}{2} \displaystyle\sum_{m=-\infty}^{\infty} H_m^{(1)}(k\rho)J_m'(kR)\cos(m(\theta-\phi)), & \rho > R \end{cases}, \tag{11}$$

$$L(s,x) = \begin{cases} L^I(s,x) = \dfrac{-\pi k i}{2} \displaystyle\sum_{m=-\infty}^{\infty} J_m'(k\rho)H_m^{(1)}(kR)\cos(m(\theta-\phi)), & R > \rho \\[2em] L^E(s,x) = \dfrac{-\pi k i}{2} \displaystyle\sum_{m=-\infty}^{\infty} H_m'^{(1)}(k\rho)J_m(kR)\cos(m(\theta-\phi)), & \rho > R \end{cases}, \tag{12}$$

$$M(s,x) = \begin{cases} M^I(s,x) = \dfrac{-\pi k^2 i}{2} \displaystyle\sum_{m=-\infty}^{\infty} J_m'(k\rho)H_m'^{(1)}(kR)\cos(m(\theta-\phi)), & R \geq \rho \\[2em] M^E(s,x) = \dfrac{-\pi k^2 i}{2} \displaystyle\sum_{m=-\infty}^{\infty} H_m'^{(1)}(k\rho)J_m'(kR)\cos(m(\theta-\phi)), & \rho > R \end{cases}, \tag{13}$$

where $i^2 = -1$, I and E denote the interior and exterior cases for the expressions of kernel, respectively. It is noted that the degenerate kernels for T and L expression for $\rho = R$ are not given since they are not continuous across the boundary. In order to fully utilize the geometry of circular boundary, the potential u and its normal flux t can be approximated

6   *J. T. Chen, C. T. Chen & I. L. Chen*

by employing the Fourier series. Therefore, we obtain

$$u(s) = a_0 + \sum_{n=1}^{\infty} (a_n \cos n\theta + b_n \sin n\theta), \quad s \in B \tag{14}$$

$$t(s) = p_0 + \sum_{n=1}^{\infty} (p_n \cos n\theta + q_n \sin n\theta), \quad s \in B \tag{15}$$

where a_0, a_n, b_n, p_0, p_n and q_n are the Fourier coefficients and θ is the polar angle which is equally discretized. Equations (8) and (9) can be easily calculated by employing the orthogonal property of Fourier series. In the real computation, only the finite M terms are used in the summation of Eqs. (14) and (15).

2.4. *Adaptive observer system*

Since the boundary integral equations are frame indifferent, *i.e.* rule of objectivity is obeyed. Adaptive observer system is chosen to fully employ the property of degenerate kernels. Figure 2 shows the boundary integration for the circular boundaries. It is worthy noted that the origin of the observer system can be adaptively located on the center of the corresponding circle under integration to fully utilize the geometry of circular boundary. The dummy variable in the integration on the circular boundary is just the angle (θ) instead of the radial coordinate (R). By using the adaptive system, all the boundary integrals can be determined analytically free of principal value.
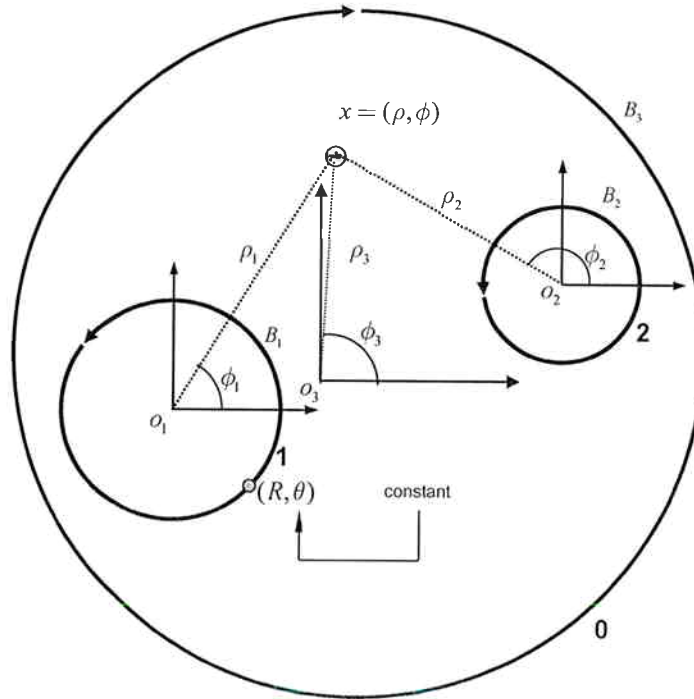
Fig. 2. Adaptive observer system.

2.5. *Vector decomposition technique for the potential gradient in the hypersingular formulaion*

Since the hypersingular equation is a key ingredient to deal with spurious eigenvalues, potential gradient on the boundary is required to calculate. For the eccentric case, the field point and source point may not locate on the circular boundaries with the same center except the two points on the same circular boundary or on the annular cases. Special treatment for the normal derivative should be taken care. As shown in Fig. 3(a) where the origins of

$\hat{e}_1$: True normal direction
$\hat{e}_2$: True tangential direction
$\hat{e}_3$: Radial derivative direction
$\hat{e}_4$: Angle derivative direction

(a) Eccentric case.

$\hat{e}_1$: True normal direction
$\hat{e}_2$: True tangential direction
$\hat{e}_3$: Radial derivative direction
$\hat{e}_4$: Angle derivative direction
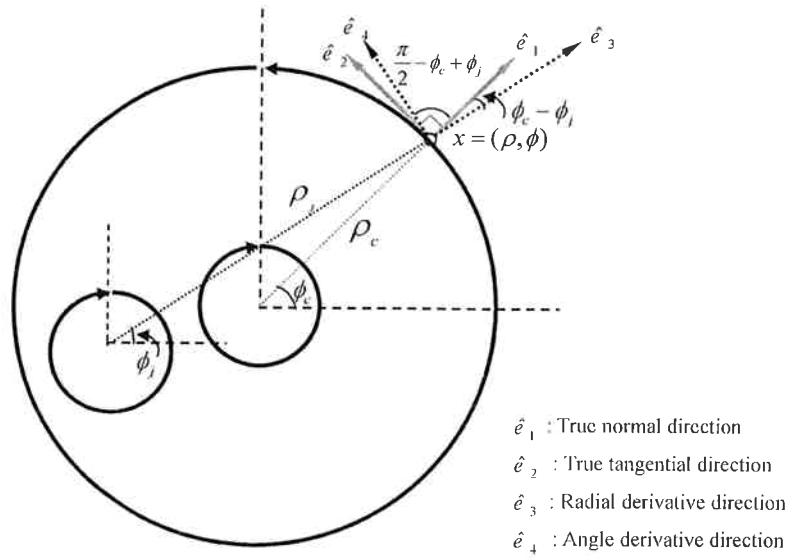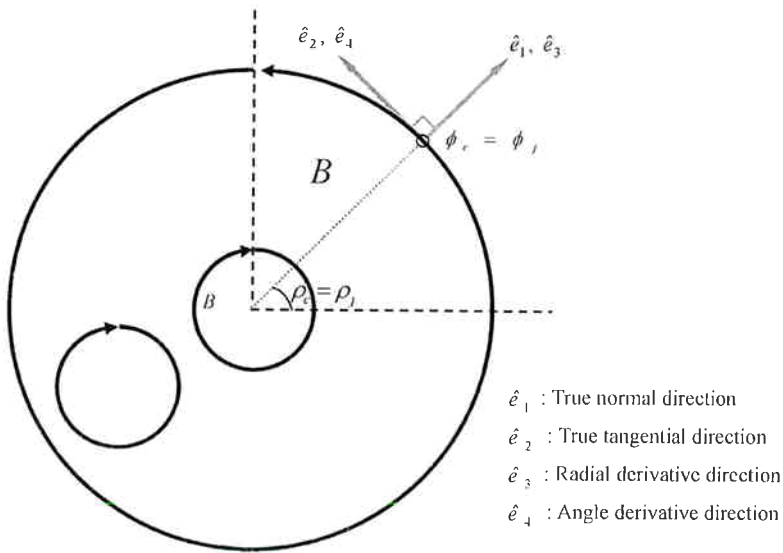
(b) Annular case.

Fig. 3. Vector decomposition for potential gradient in the hypersingular equation.

observer system are different, the true normal direction $\hat{e}_1$ with respect to the collocation point x on the B_j boundary should be superimposed by using the radial direction $\hat{e}_3$ and angular direction $\hat{e}_4$. We call this treatment "vector decomposition technique". According to the concept, Eqs. (12) and (13) can be modified as

$$L(s,x) = \begin{cases} L^I(s,x) = \dfrac{-\pi k i}{2} \displaystyle\sum_{m=-\infty}^{\infty} J_m(k\rho)H_m^{(1)}(kR)\cos(m(\theta-\phi))\cos(\phi_c-\phi_j) \\ \qquad\qquad -\dfrac{m}{k\rho}J_m(k\rho)H_m^{(1)}(kR)\sin(m(\theta-\phi))\sin(\phi_c-\phi_j), \quad R>\rho \\[2mm] L^E(s,x) = \dfrac{-\pi k i}{2} \displaystyle\sum_{m=-\infty}^{\infty} H_m^{(1)}(k\rho)J_m(kR)\cos(m(\theta-\phi))\cos(\phi_c-\phi_j) \\ \qquad\qquad -\dfrac{m}{k\rho}J_m(k\rho)H_m^{(1)}(kR)\sin(m(\theta-\phi))\sin(\phi_c-\phi_j), \quad \rho>R \end{cases}$$

$$(16)$$

$$M(s,x) = \begin{cases} M^I(s,x) = \dfrac{-\pi k i}{2} \displaystyle\sum_{m=-\infty}^{\infty} J_m(k\rho)H_m^{(1)}(kR)\cos(m(\theta-\phi))\cos(\phi_c-\phi_j) \\ \qquad\qquad -\dfrac{m}{k\rho}J_m(k\rho)H_m'^{(1)}(kR)\sin(m(\theta-\phi))\sin(\phi_c-\phi_j), \quad R\geq\rho \\[2mm] M^E(s,x) = \dfrac{-\pi k i}{2} \displaystyle\sum_{m=-\infty}^{\infty} H_m'^{(1)}(k\rho)J_m(kR)\cos(m(\theta-\phi))\cos(\phi_c-\phi_j) \\ \qquad\qquad -\dfrac{m}{k\rho}J_m(k\rho)H_m'^{(1)}(kR)\sin(m(\theta-\phi))\sin(\phi_c-\phi_j), \quad \rho>R \end{cases}$$

$$(17)$$

For the annular case as shown in Fig. 3(b), the true normal direction $\hat{e}_1$ on the boundary is nothing but the radial derivative $\hat{e}_3$. The angular derivative $\hat{e}_4$ is perpendicular to the normal direction $\hat{e}_1$.

2.6. *Linear algebraic equation*

In order to calculate the $2M+1$ unknown Fourier coefficients, $2M+1$ boundary points on each circular boundary are needed to be collocated. By collocating the null-field point exactly on the kth circular boundary for Eqs. (8) and (9) as shown in Fig. 4(a), we have

$$0 = \sum_{j=0}^{N_c} \int_{B_j} T(s,x_j)u(s)dB(s) - \sum_{j=0}^{N_c} \int_{B_j} U(s,x_j)t(s)dB(s), \quad x_j \in D^e \cup B \qquad (18)$$

$$0 = \sum_{j=0}^{N_c} \int_{B_j} M(s,x_j)u(s)dB(s) - \sum_{j=0}^{N_c} \int_{B_j} L(s,x_j)t(s)dB(s), \quad x_k \in D^e \cup B \qquad (19)$$

where N_c is the number of inner circles and the path is anticlockwise for the outer circle. Otherwise, it is clockwise. It is noted that Eqs. (18) and (19) are also valid for $x \in B$ since
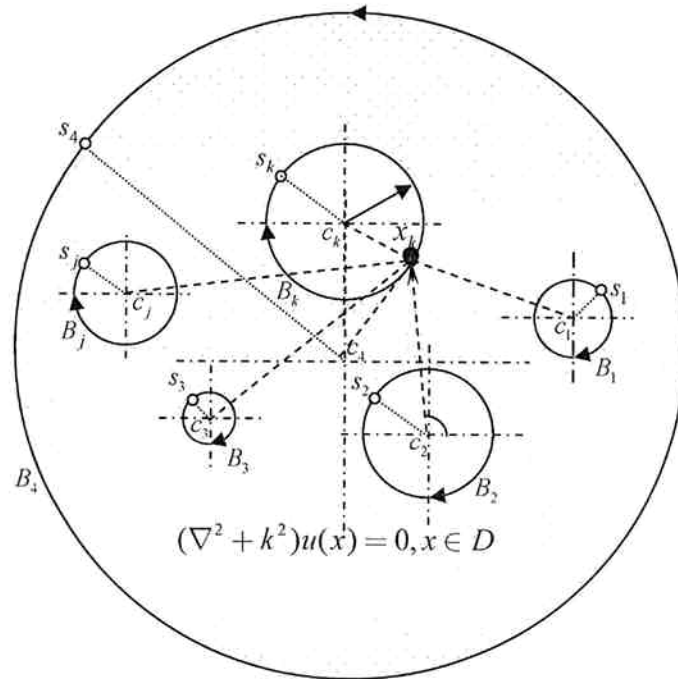
(a) Null-field integral equation. (x move to B from D^e).
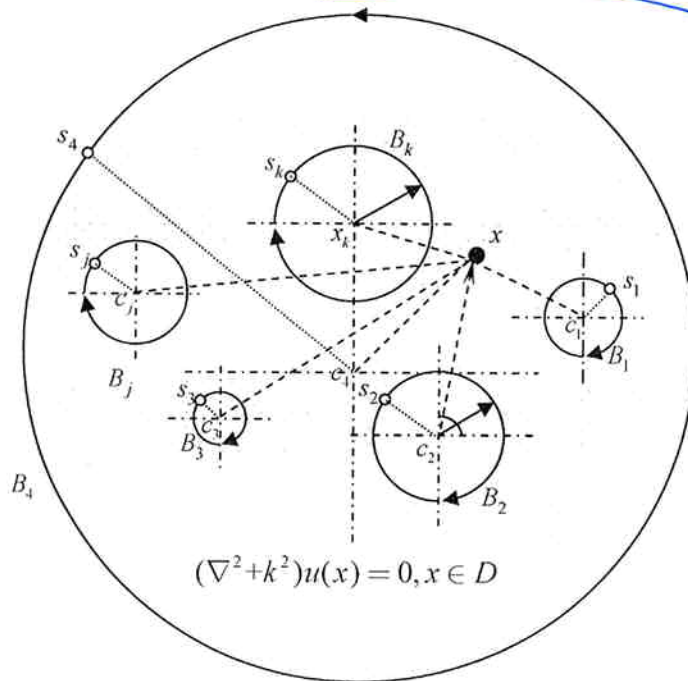
(b) Boundary integral equation for the domain point.

Fig. 4. Boundary integral formulation.

10   *J. T. Chen, C. T. Chen & I. L. Chen*

the appropriate kernel expression is adopted. For the B_j integral of the circular boundary, the kernels of $U(s,x)$, $T(s,x)$, $L(s,x)$ and $M(s,x)$ are respectively expressed in terms of degenerate kernels of Eqs. (10), (11), (16) and (17) with respect to the observer origin at the center of B_j. The boundary densities of $u(s)$ and $t(s)$ are substituted by using the Fourier series of Eqs. (14) and (15), respectively. In the B_j integration, we set the origin of the observer system to collocate at the center c_j of B_j to fully utilize the degenerate kernel and Fourier series. By collocating the null-field point which can be much close to the boundary B_j from outside of the domain, a linear algebraic system is obtained

$$[\mathbf{U}]\{\mathbf{t}\} = [\mathbf{T}]\{\mathbf{u}\} \tag{20}$$

$$[\mathbf{L}]\{\mathbf{t}\} = [\mathbf{M}]\{\mathbf{u}\} \tag{21}$$

where $[\mathbf{U}]$, $[\mathbf{T}]$, $[\mathbf{L}]$ and $[\mathbf{M}]$ are the influence matrices with a dimension of $N \times (2M+1)$ by $N \times (2M+1)$ and $\{\mathbf{t}\}$ and $\{\mathbf{u}\}$ denote the vectors for $t(s)$ and $u(s)$ of the Fourier coefficients with a dimension of $N \times (2M+1)$ by 1. For simplicity, the Dirichlet case of $u(s) = 0$ is considered. We can obtain the nonlinear characteristic equation as follows,

$$[\mathbf{U}]\{\mathbf{t}\} = \{0\}, \tag{22}$$

$$[\mathbf{L}]\{\mathbf{t}\} = \{0\}, \tag{23}$$

where, $[\mathbf{U}]$, $[\mathbf{L}]$ and $\{\mathbf{t}\}$ can be defined as follows:

$$[\mathbf{U}] = \begin{bmatrix} \mathbf{U}_{00} & \mathbf{U}_{01} & \cdots & \mathbf{U}_{0N_c} \\ \mathbf{U}_{10} & \mathbf{U}_{11} & \cdots & \mathbf{U}_{1N_c} \\ \vdots & \vdots & \ddots & \vdots \\ \mathbf{U}_{N_c0} & \mathbf{U}_{N_c0} & \cdots & \mathbf{U}_{NN_c} \end{bmatrix}, \quad [\mathbf{L}] = \begin{bmatrix} \mathbf{L}_{00} & \mathbf{L}_{01} & \cdots & \mathbf{L}_{0N_c} \\ \mathbf{L}_{10} & \mathbf{L}_{11} & \cdots & \mathbf{L}_{1N_c} \\ \vdots & \vdots & \ddots & \vdots \\ \mathbf{L}_{N_c0} & \mathbf{L}_{N_c0} & \cdots & \mathbf{L}_{N_cN_c} \end{bmatrix}, \tag{24}$$

$$\{\mathbf{t}\} = \begin{Bmatrix} \mathbf{t}_0 \\ \mathbf{t}_1 \\ \mathbf{t}_2 \\ \vdots \\ \mathbf{t}_N \end{Bmatrix}, \tag{25}$$

where the vectors $\{\mathbf{t}_j\}$ is in the form of $\{p_0^j p_1^j q_1^j \cdots p_M^j q_M^j\}^T$ and $[\mathbf{U}_{ij}]$ denotes the influence matrix. The first subscript "i" ($i = 0, 1, 2, \ldots, N_c$) in the $[\mathbf{U}_{ij}]$ denotes the index of the ith circle where the collocation point is located and the second subscript "j" ($j = 0, 1, 2, \ldots, N_c$) denotes the index of the jth circle where the boundary data $\{\theta_j\}$ are specified. N_c is the number of circular holes in the domain and M indicates the highest harmonic of truncated terms in Fourier series. The coefficient matrix of the linear algebraic system is partitioned into blocks, and each diagonal block (U_{jj}) corresponds to the influence matrices due to the same circle of collocation and Fourier expansion. After uniformly collocating the point along

the ith circular boundary, the submatrix can be written as

$$[U_{ij}] = \begin{bmatrix} U_{ij}^{0c}(\phi_1) & U_{ij}^{1c}(\phi_1) & U_{ij}^{1s}(\phi_1) & \cdots & U_{ij}^{Mc}(\phi_1) & U_{\alpha\beta}^{Ms}(\phi_1) \\ U_{ij}^{0c}(\phi_2) & U_{ij}^{1c}(\phi_2) & U_{ij}^{1s}(\phi_2) & \cdots & U_{ij}^{Mc}(\phi_2) & U_{\alpha\beta}^{Ms}(\phi_2) \\ U_{ij}^{0c}(\phi_3) & U_{ij}^{1c}(\phi_3) & U_{ij}^{1s}(\phi_3) & \cdots & U_{ij}^{Mc}(\phi_3) & U_{\alpha\beta}^{Ms}(\phi_3) \\ \vdots & \vdots & \vdots & \ddots & \vdots & \vdots \\ U_{ij}^{0c}(\phi_{2M}) & U_{ij}^{1c}(\phi_{2M}) & U_{ij}^{1s}(\phi_{2M}) & \cdots & U_{ij}^{Mc}(\phi_{2M}) & U_{\alpha\beta}^{Ms}(\phi_{2M}) \\ U_{ij}^{0c}(\phi_{2M+1}) & U_{ij}^{1c}(\phi_{2M+1}) & U_{ij}^{1s}(\phi_{2M+1}) & \cdots & U_{ij}^{Mc}(\phi_{2M+1}) & U_{\alpha\beta}^{Ms}(\phi_{2M+1}) \end{bmatrix} \tag{26}$$

$$[L_{ij}] = \begin{bmatrix} L_{ij}^{0c}(\phi_1) & L_{ij}^{1c}(\phi_1) & L_{ij}^{1s}(\phi_1) & \cdots & L_{ij}^{Mc}(\phi_1) & L_{\alpha\beta}^{Ms}(\phi_1) \\ L_{ij}^{0c}(\phi_2) & L_{ij}^{1c}(\phi_2) & L_{ij}^{1s}(\phi_2) & \cdots & L_{ij}^{Mc}(\phi_2) & L_{\alpha\beta}^{Ms}(\phi_2) \\ L_{ij}^{0c}(\phi_3) & L_{ij}^{1c}(\phi_3) & L_{ij}^{1s}(\phi_3) & \cdots & L_{ij}^{Mc}(\phi_3) & L_{\alpha\beta}^{Ms}(\phi_3) \\ \vdots & \vdots & \vdots & \ddots & \vdots & \vdots \\ L_{ij}^{0c}(\phi_{2M}) & L_{ij}^{1c}(\phi_{2M}) & L_{ij}^{1s}(\phi_{2M}) & \cdots & L_{ij}^{Mc}(\phi_{2M}) & L_{\alpha\beta}^{Ms}(\phi_{2M}) \\ L_{ij}^{0c}(\phi_{2M+1}) & L_{ij}^{1c}(\phi_{2M+1}) & L_{ij}^{1s}(\phi_{2M+1}) & \cdots & L_{ij}^{Mc}(\phi_{2M+1}) & L_{\alpha\beta}^{Ms}(\phi_{2M+1}) \end{bmatrix} \tag{27}$$

where ϕ_m, $m = 1, 2, \ldots, 2M + 1$ is the polar angle of the collocating points x_m around boundary. It is noted that the superscript "0s" in Eq. (26) disappears since $\sin 0\theta = 0$. And the element of $[U_{ij}]$ and $[L_{ij}]$ are defined as

$$U_{ij}^{nc}(\phi_m) = \int_{B_j} U(s_j, x_m) \cos(n\theta_j) R_j d\theta_j, \quad n = 0, 1, 2, \ldots, M, \tag{28}$$

$$U_{ij}^{ns}(\phi_m) = \int_{B_j} U(s_j, x_m) \sin(n\theta_j) R_j d\theta_j, \quad n = 0, 1, 2, \ldots, M, \tag{29}$$

$$L_{ij}^{nc}(\phi_m) = \int_{B_j} L(s_j, x_m) \cos(n\theta_j) R_j d\theta_j, \quad n = 0, 1, 2, \ldots, M, \tag{30}$$

$$L_{ij}^{ns}(\phi_m) = \int_{B_j} L(s_j, x_m) \sin(n\theta_j) R_j d\theta_j, \quad n = 0, 1, 2, \ldots, M, \tag{31}$$

where ϕ_m is in the ith circle. By employing the direct-searching scheme, SVD technique can obtain the eigenvalues and boundary mode at the same time. After obtaining the eigenvalues and unknown Fourier coefficients, the origin of observer system is set to c_j in the B_j integration as shown in Fig. 4(b) to obtain the interior potential by employing Eq. (2). The difference with BEM is shown in Table 1.

12   *J. T. Chen, C. T. Chen & I. L. Chen*

Table 1. The difference between the present method and BEM, where RPV, CPV and HPV denote Riemann principle value, Cauchy principle value and Hardmard principle value.

Method	Boundary Density Discretization	Auxiliary System	Coordinate System	Boundary Integral	Formulation
Present method	$u(\theta)$ or $t(\theta)$	Degenerate kernel	Adaptive observer system	No principal Value	Null-field integral equations
BEM	$u(\theta)$ or $t(\theta)$	Fundamental solution	Fixed observer system	Principal values (CPV, RPV and HPV)	Boundary integral equation for boundary point

3. Discussions on Spurious Eigenvalues

For the multiply-connected eigenproblem with an inner circular boundary of radius a, Eq. (22) yields

$$
\begin{bmatrix}
\cdots & J_0(ka)H_0(k\rho_0) & \cdots & J_M(ka)H_M(k\rho_0)\cos M\phi_1 & J_M(ka)H_M(k\rho_0)\sin M\phi_1 & \cdots \\
\cdots & J_0(ka)H_0(k\rho_1) & \cdots & J_M(ka)H_M(k\rho_1)\cos M\phi_2 & J_M(ka)H_M(k\rho_1)\sin M\phi_2 & \cdots \\
\cdots & \vdots & \ddots & \vdots & \vdots & \cdots \\
\cdots & J_0(ka)H_0(k\rho_M) & \cdots & J_M(ka)H_M(k\rho_M)\cos M\phi_{2M+1} & J_M(ka)H_M(k\rho_M)\sin M\phi_{2M+1} & \cdots \\
\hdashline
\cdots & J_0(ka)H_0(ka) & \cdots & J_M(ka)H_M(ka)\cos M\phi_1 & J_M(ka)H_M(ka)\sin M\phi_1 & \cdots \\
\cdots & J_0(ka)H_0(ka) & \cdots & J_M(ka)H_M(ka)\cos M\phi_2 & J_M(ka)H_M(ka)\sin M\phi_2 & \cdots \\
\cdots & \vdots & \ddots & \vdots & \vdots & \cdots \\
\cdots & J_0(ka)H_0(ka) & \cdots & J_M(ka)H_M(ka)\cos M\phi_{2P+1} & J_M(ka)H_M(ka)\sin M\phi_{2M+1} & \cdots
\end{bmatrix}
\begin{Bmatrix}
p_0^1 \\ \vdots \\ p_M^1 \\ q_M^1 \\ \hdashline p_0^2 \\ \vdots \\ p_M^2 \\ q_M^2
\end{Bmatrix} = 0
\tag{32}
$$

for the Dirichlet problems by using the singular formulation. The determinant of the influence matrix is zero for $J_m(ka) = 0$, $m = 0, 1, 2, 3, \ldots, M$ for Eq. (32). Similarly, the hypersingular equation the determinant is zero for $J'_m(ka) = 0$, $m = 0, 1, 2, 3, \ldots, M$. It indicates that the eigenvalue for the Dirichlet problems of circular domain with the radius a, is the possible eigenvalue in the UT formulation for the considered multiply-connected problem. The possible eigenvalues of $J_m(ka) = 0$ and $J'_m(ka) = 0$, $m = 0, 1, 2, 3, \ldots, M$ are found to be the true eigenvalues of a circular domain with radius a subject to the Dirichlet and Neumann boundary conditions, respectively. However, they are not true eigenvalues of the multiply-connected domain problems. This is the reason why we term them spurious eigenvalues. This finding extends the proof of existence of spurious eigenvalues for the annular

case[10] by using circulants and degenerate kernels. We can claim that any inner circle results in the spurious eigenvalue for the multiply-connected eigenproblems. The spurious eigenvalues are found to be the true eigenvalues of the associated eigenproblem of inner circles. To overcome the spurious eigenvalues, we use the Burton & Miller method and SVD updating technique.

4. Burton & Miller Method and SVD Updating Technique Review

4.1. *Burton & Miller method*

In the exterior acoustics, Burton & Miller utilized the product of hypersingular equation with an imaginary constant to the singular equation to deal with fictitious frequency which is the non-uniqueness solution problem. We will extend this concept to suppress the appearance of spurious eigenvalues for multiply-connected problems. By combining the two equations (25) and (26) using Burton & Miller approach, the linear algebraic equations can be obtained as follows:

$$[ikU(s,x) + L(s,x)]\{t\} = [ikT(s,x) + M(s,x)]\{u\}. \tag{33}$$

Equation (38) is valid for filitering out the spurious eigensolutions in the multiply-connected problem.

4.2. *SVD updating techniques*

By employing the UT and LM formulations, we have the Eqs. (20) and (21). A conventional approach to detect the nonunique solution is the criterion of satisfying both Eqs. (20) and (21) at the same time. The *UT* or *LM* method in conjunction with SVD techniques can filter out the spurious eigenvalues for multiply-connected problems. Employing the SVD technique, one can decompose Eq. (20) into

$$\phi_T \sum_T \psi_T^H \{u\} = \phi_U \sum_U \psi_U^H \{t\}, \tag{34}$$

where H denotes the Hermitian conjugate, ϕ_U, ψ_U, ϕ_T and ψ_T are the unitary matrices, $\sum_U$ and $\sum_T$ are the diagonal matrices composed by the singular values $\sigma_i^{(U)}$ and $\sigma_i^{(T)}$ of U and T matrices, respectively. When k is a spurious eigenvalue (k_s), there exists a ϕ_s vector which satisfies

$$[U^H(k_s)]\{\phi_s\} = 0, \tag{35}$$

and

$$[T^H(k_s)]\{\phi_s\} = 0, \tag{36}$$

respectively. Combining Eqs. (35) and (36), we have

$$\begin{bmatrix} U^H(k_s) \\ T^H(k_s) \end{bmatrix} \{\phi_s\} = 0. \tag{37}$$

14   *J. T. Chen, C. T. Chen & I. L. Chen*

In order to verify the existence of vectorϕ_s, we can employ the Fredholm alternative theorem.[1] By taking the Hermitian conjugate with respect to Eq. (37), we have

$$\{\phi_s\}^H [U(k_s)T(k_s)] = 0, \tag{38}$$

where ϕ_s is the spurious boundary mode encountered in the "singular" equation. The assemble of U and T matrices in Eqs. (37) and (38) are found to be the SVD updating terms and documents, respectively. It will be found that the spurious modes can be extracted out from the left unitary vector in U and T matrices. Similarly, Eqs. (37) and (38) can be rewritten by replacing the U and T matrices into L and M matrices, respectively, when using hypersingular equation. In a similar way, the spurious boundary mode can be extracted out from the left unitary vector in L and M matrices. According to the Eqs. (22) and (23), for extracting out the true eigensolution we can merge the two matrices of U and L together to obtain an overdeterminated system,

$$\begin{bmatrix} U \\ L \end{bmatrix} \{t\} = 0, \tag{39}$$

for the Dirichlet type problem ($u = 0$). Consequently, the SVD techniques of updating term is also employed in the overdeterminated matrix of Eq. (44) to find the true eigenvalues and true boundary modes. The right unitary vectors in SVD[1] for U and L kernel corresponding to the zero singular value are found to be the true boundary eigenvectors.

5. Numerical Results and Discussion

In order to demonstrate the validity of the present method, several examples are given.

Example 1. Membrane vibration for a circular domain with an annular circular hole

An annular case with radii r_1 and r_2 ($r_1 = 0.5, r_2 = 2.0$) is shown in Fig. 5. The Dirichlet boundary condition is considered. Table 2 shows the former five true eigenvalues by using different methods for comparison with analytical solution. It can be found that the present result is acceptable. Chen *et al.*[15] had proved by using the singular value decomposition (SVD) technique that both the singular and hypersingular equations result in spurious eigenvlaues which are the associated interior Dirichlet and Neumann problems of interior domain of ineer circles, respectively. Figure 6(a) shows the minimum singular value versus k where the drop indicates the possible eigenvalues by using the singular formulation, it is found that the accuracy of present method is better than that of BEM. Figure 6(b) shows the minimum singular value versus k where the drop indicates the possible eigenvalues by using the hypersingular formulation. It is found in Fig. 6(b) that the zero spurious eigenvalue is well shown than BEM where $k = 0.34$ is predicted. This indicates that the low frequency behavior is better modeled by using the present method than BEM. Figure 6(c) shows the minimum singular value versus k where the drop indicates all the true eigenvalues by employing the Burton & Miller approach. The present method by using the singular formulation agree with the analytical results better than BEM[10] does where a spurious
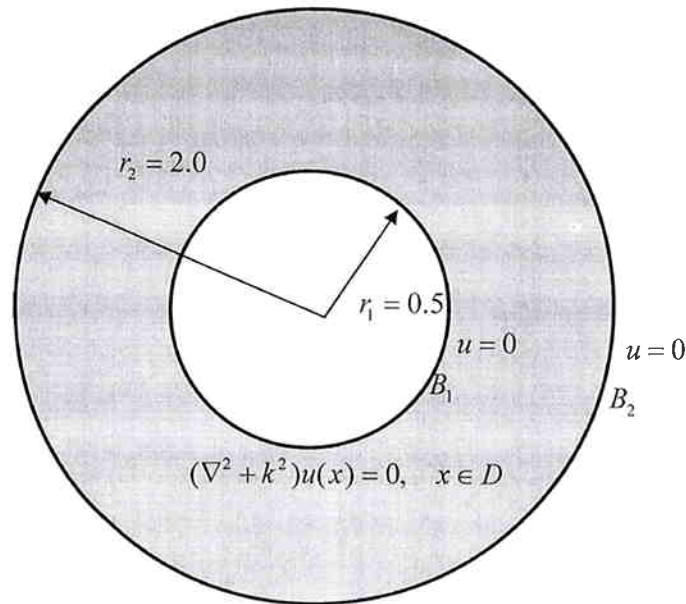
Fig. 5. Eigenproblem with an annular domain.

Table 2. The former five eigenvalues of the Helmholtz eigenproblem for the annular cavity.

Methods	Eigenvalues					
	k_1	k_2	k_3	k_4		k_5
FEM[1] (ABAQUS)	2.03	2.20	2.62	3.15		3.71
BEM[1] (Burton & Miller)	2.06	2.23	2.67	3.22		3.81
BEM[9] (CHIEF)	2.05	2.23	2.67	3.22		3.81
BEM[9] (null-field)	2.04	2.20	2.65	3.21		3.80
BEM[9] (fictitious)	2.04	2.21	2.66	3.21		3.80
Present method	2.05	2.22	2.66	3.21		3.80
Analytical solution[9]	2.05	2.23	2.66	3.21		3.80

eigenvalue appears at $k = 4.81$ ($J_0(4.81r_1) = 0$) instead of 4.83 in BEM. The present method by using the hypersingular formulation agree with the analytical solution better than BEM[10] does where a spurious eigenvalue appears at $k = 0.0$ and $3.68(J_0^1(0r_1) = 0$ $J_0^1(0r_1) = 0$ and $J_0^2(3.68r_1) = 0$ where the superscript "1" and "2" mean the first and second roots) instead of 0.34 and 3.68 in BEM. The present method is superior to BEM especially in the low frequency range and it is more accurate than BEM under the same number of degree of freedoms. In order to filter out spurious eigenvalues, the Burton & Miller method is utilized as shown in Fig. 6(c). It is found that only true eigenvalues exist and spurious eigenvalues are filtered out.[10] By adopting the truncated Fourier series (M = 10), the former five mode shapes are compared well with FEM and BEM shown in Table 3.
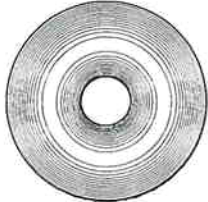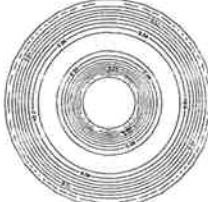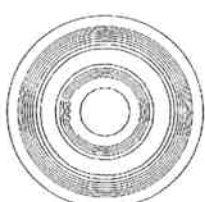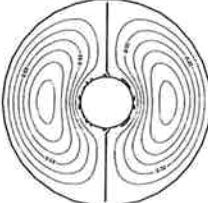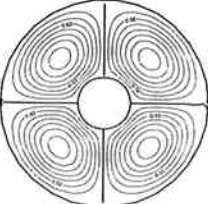
16   *J. T. Chen, C. T. Chen & I. L. Chen*
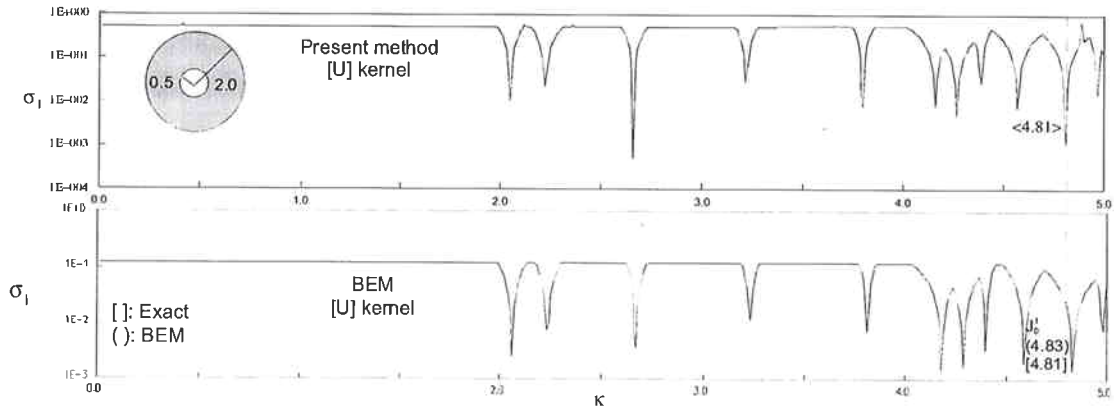
(a) U kernel.
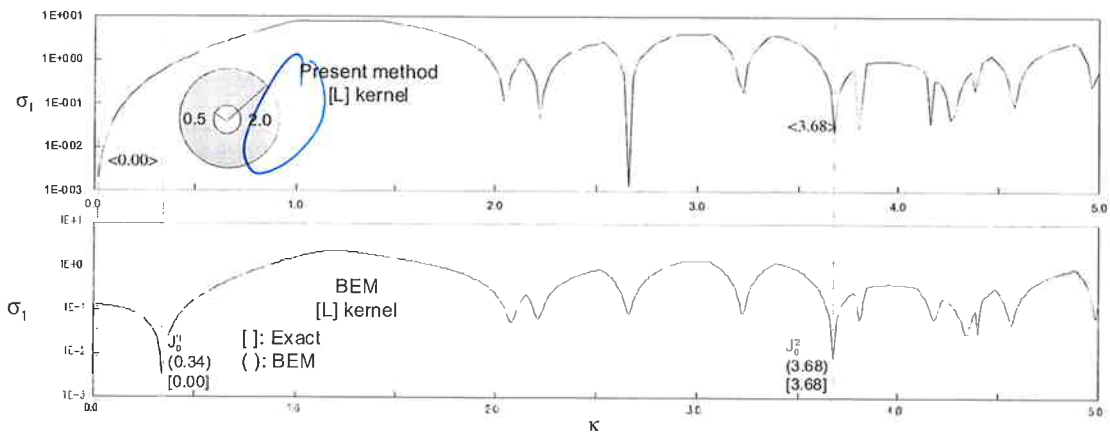
(b) L kernel.
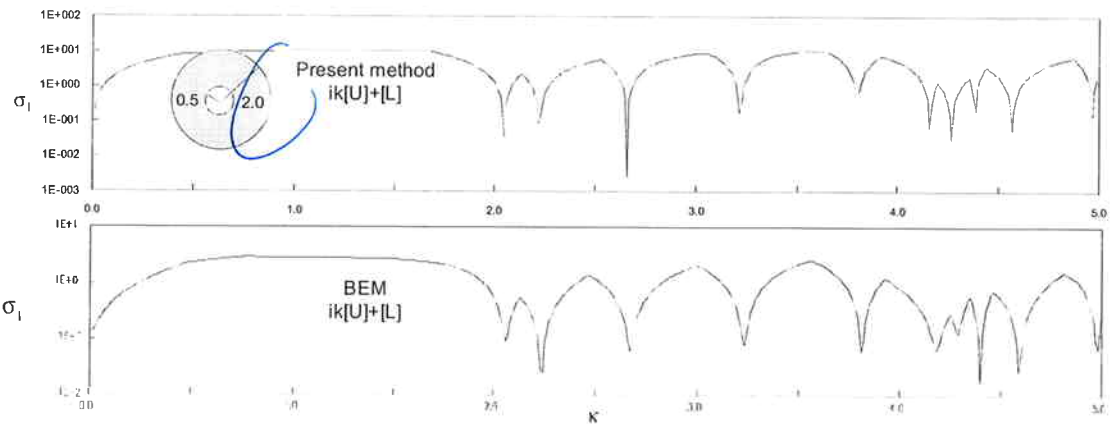
(c) $(ikU + L)$ kernel (Burton & Miller approach).

Fig. 6. The minimim singular value σ_1 versus k for the Dirichlet annular problem by using the present method and BEM.

Table 3. The former three eigenmodes for the annular case by using the present method, FEM and BEM.

Mode	Present method ($M = 10$)	BEM[10]	FEM[10]
1	$k = 2.05$	$k = 2.06$	$k = 2.03$
2	$k = 2.22$	$k = 2.23$	$k = 2.20$
3	$k = 2.66$	$k = 2.67$	$k = 2.62$

Example 2. Membrane vibration for a circular domain with an eccentric circular hole.

An eccentric case with radii r_1 and r_2 ($r_1 = 0.5$, $r_2 = 2.0$) is considered as shown in Fig. 7. The boundary condition is subject to the Dirichlet type. Special treatment for vector decompositions in potential gradient should be taken care here. Table 4 shows the former five eigenvalues by using different methods. Good agreement is made. Figure 8(a) shows the minimum singular value versus k where the drop indicates the possible eigenvalues by using the singular formulation. Figure 8(b) shows the minimum singular value versus k where the drop indicates the possible eigenvalues by using the hypersingular formulation. As the same with the *example* 1, the efficiency and accuracy of the present method is obviously shown in Figs. 8(a) and 8(b). Figure 8(c) shows the minimum singular value versus k where the drop indicates all the true eigenvalues by using the Burton & Miller approach. The present method by using the singular formulation agree with the analytical results better than BEM[10] does where a spurious eigenvalue appears at $k = 4.81$ ($J_0(4.81r_1) = 0$) instead of 4.83 in BEM. The present method by using the hypersingular formulation agree with the analytical solution better than BEM[10] does where a spurious eigenvalue appears at
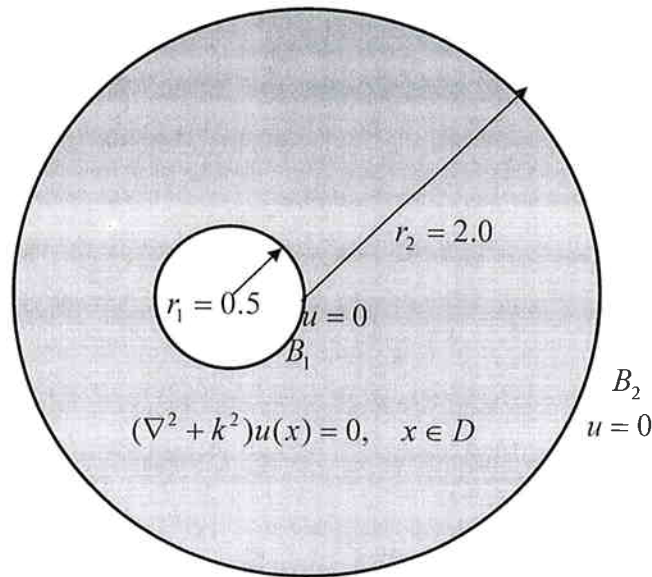
Fig. 7. Eigenproblem with an eccentric domain.

Table 4. The former five eigenvalues for an eccentric domain by using different methods.

Method	Wave Number				
	1	2	3	4	5
FEM[33]	1.73	2.13	2.45	2.76	2.95
Chen and Zhou[2]	1.75	2.14	2.47	2.78	2.97
BEM[32]	1.74	2.14	2.47	2.78	2.98
Present method	1.74	2.14	2.46	2.78	2.96

$k = 0.0$ and $3.68(J_0^1(0r_1) = 0$ and $J_0^2(3.68r_1) = 0)$ instead of 0.35 and 3.77 in BEM. The present method is superior to BEM especially in the low frequency range and it is more accurate than BEM under the same number of degree of freedoms. The spurious eigenvalue was filtered out by using the Burton and Miller approach.[1] By adopting the truncated Fourier series ($M = 10$), the former five mode shapes are compared well with those by FEM and BEM also shown in Table 5. For the convergence study of Fourier series, we plot the Parseval's sum versus truncated M terms in Fig. 9. The Parseval's theorem are defined as below

$$\int_0^{2\pi} f^2(\theta)d\theta \approx 2\pi a_0^2 + \pi \sum_{n=1}^{M}(a_n^2 + b_n^2). \tag{40}$$

It is found that no matter real-part, imaginary-part or absolute values are all convergent by selecting seven terms of Fourier series for both the inner and outer circles. Although

(a) U kernel.

(b) L kernel.

(c) $(ikU + L)$ kernel (Burton & Miller approach).
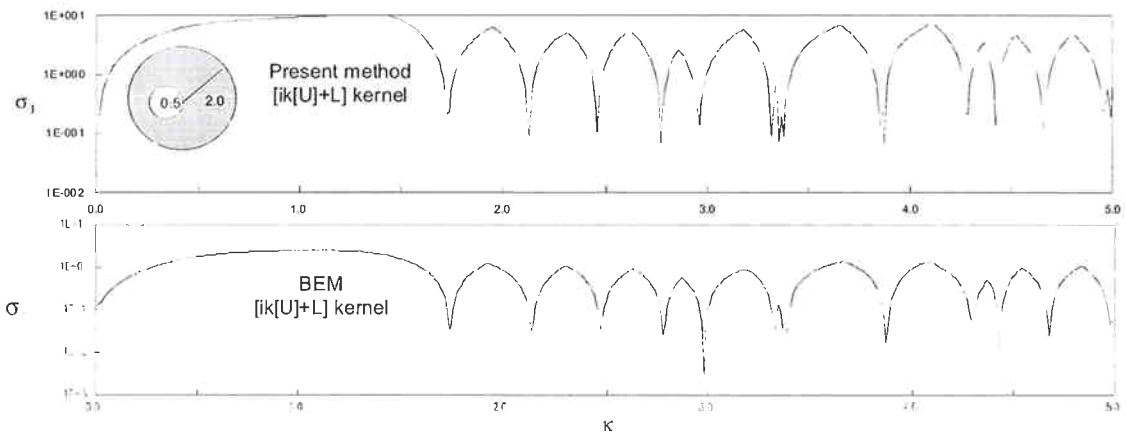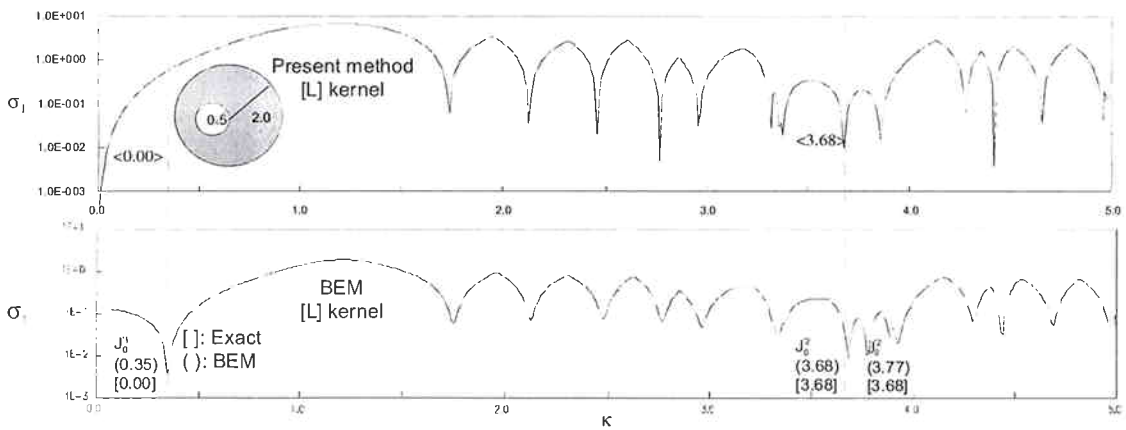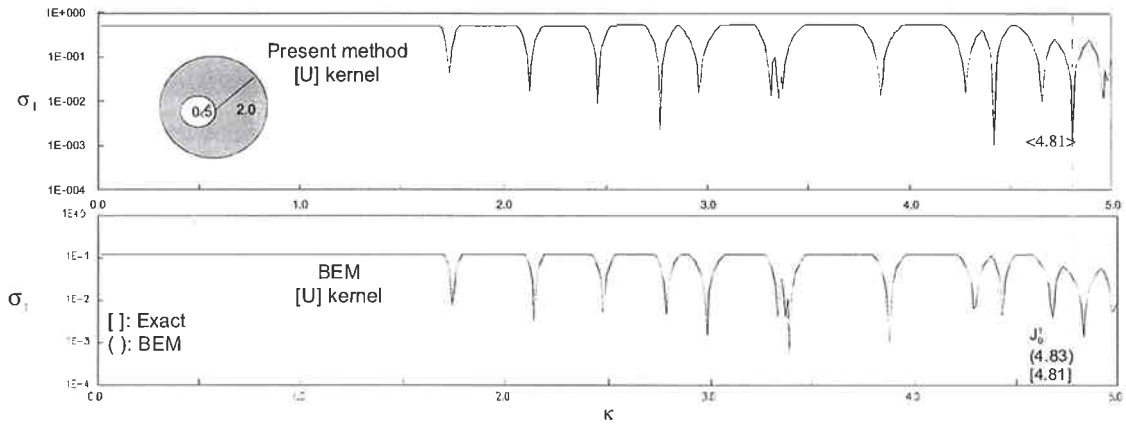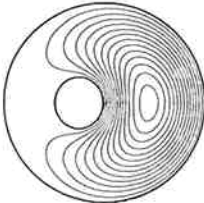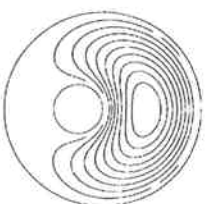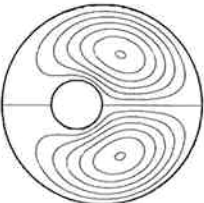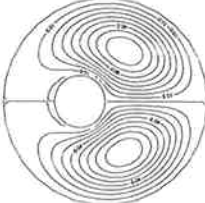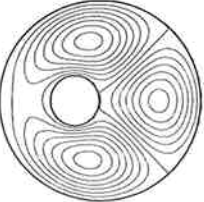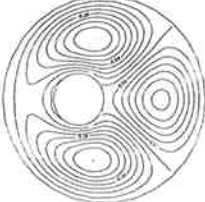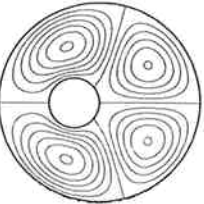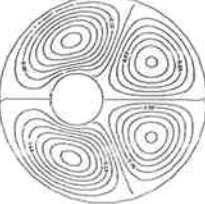
Fig. 8. The minimim sin gular value σ_1 versus k for the Dirichlet problem with an eccentric hole by using the present method and BEM.

20   *J. T. Chen, C. T. Chen & I. L. Chen*

Table 5. The former five eigenmodes for eccentric case by using the present method, FEM and BEM.

Mode	Present method ($M = 10$)	BEM[10]	FEM[10]
1	$k = 1.74$	$k = 1.74$	$k = 1.74$
2	$k = 2.14$	$k = 2.14$	$k = 2.13$
3	$k = 2.46$	$k = 2.47$	$k = 2.45$
4	$k = 2.78$	$k = 2.78$	$k = 2.76$
5	$k = 2.94$	$k = 2.97$	$k = 2.95$
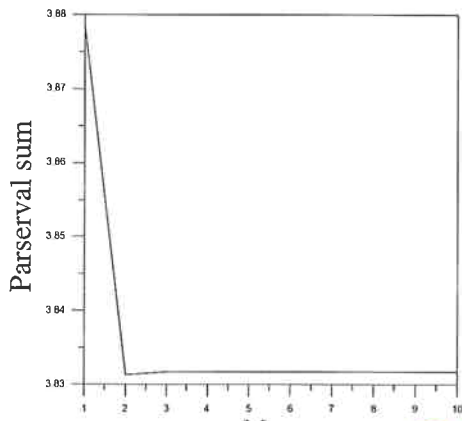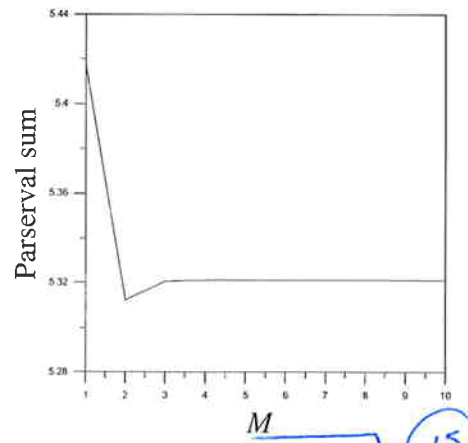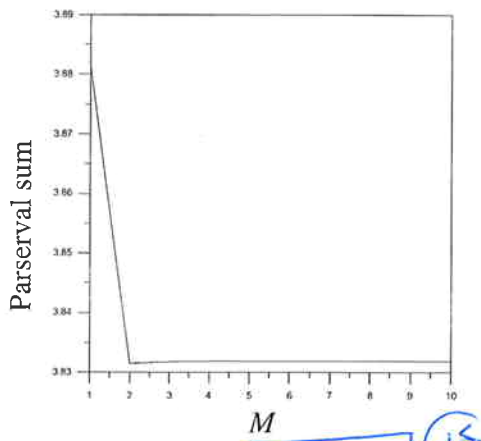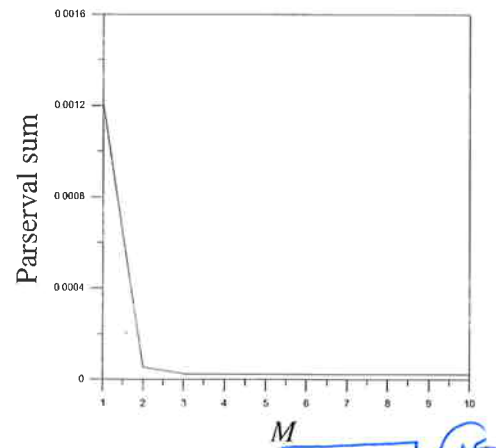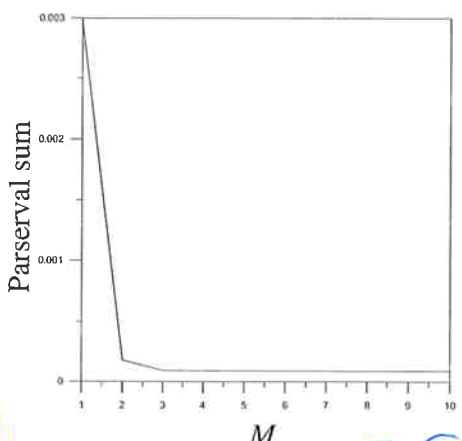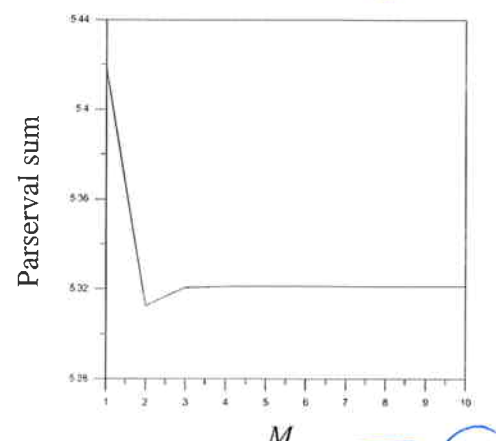
Fig. 9. The Parserval sum of t versus the truncated term M.

22   *J. T. Chen, C. T. Chen & I. L. Chen*

they are not monotonically decreasing, they converge to a value due to the constraint of the null-field integral equations.

Example 3. Membrane vibration for a circular domain with two equal circular holes.

A circular region of radius R with two equal circular with the eccentricity $e = 0.5$ are shown in Fig. 10. The radii of the circular holes and the external boundary are $c = 0.3$ and $R = 1.0$. The Dirichlet boundary condition is considered. By adopting the truncated Fourier series ($M = 10$), the former five mode shapes are compared by BEM and FEM as shown in Table 6. For the double roots, mode 1 and mode 2 are quite different. Mode 1 is symmetric with respect to the x axis, while the mode 2 is antisymmetric with respect to the x axis. The same situation is for the mode 3 and mode 4. Good agreement is made.
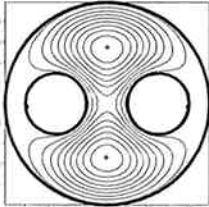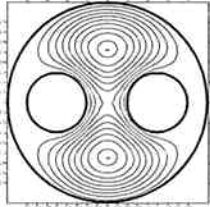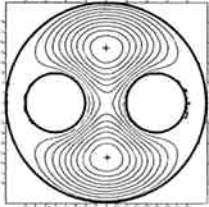
Example 4. Membrane vibration for a circular domain with two unequal circular holes.

A circular region of radius R with two unequal circular holes with the eccentricity $e = 0.5$ are shown in Fig. 11. The radii of the circular holes and the external boundary are $c1 = 0.3$, $c2 = 0.4$ and $R = 1.0$. The Dirichlet boundary condition is considered. Table 7 shows the former five eigenvalues by using different methods. Good agreement is made. The spurious eigenvalus are detected by using the present method and BEM in conjunction with SVD technique of updating document as shown in Fig. 12 where only seven terms are adopted in the Fourier series. By adopting the truncated Fourier series ($M = 10$), the former five mode shapes are compared with those by BEM and FEM as shown in Table 8. For the double roots, mode 1 and mode 2 are quite different. Mode 1 is symmetric with respect to the x axis, while the mode 2 is antisymmetric with respect to the x axis. The same situation is for the mode 3 and mode 4.
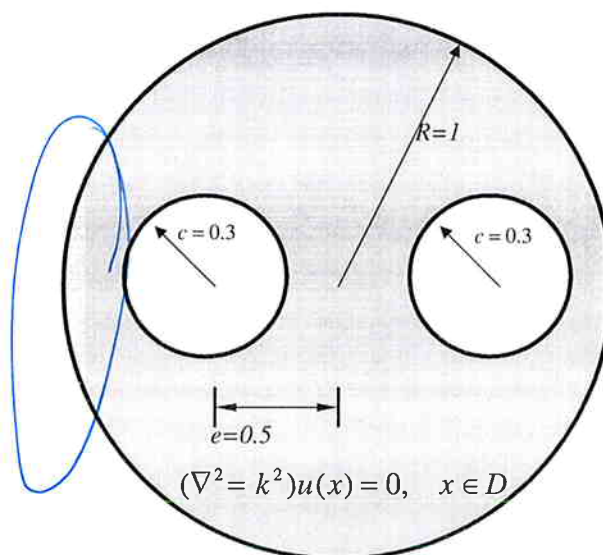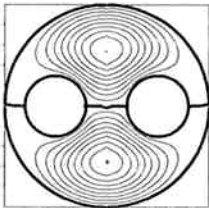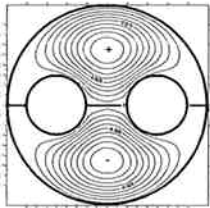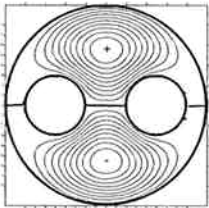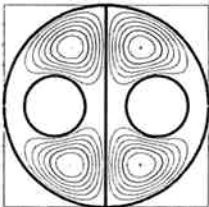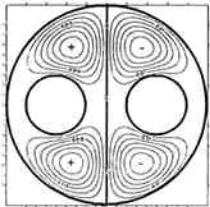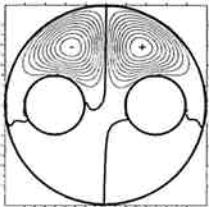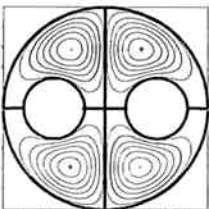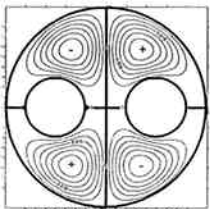
Fig. 10. Two equal circular holes in a circular domain.
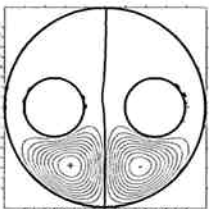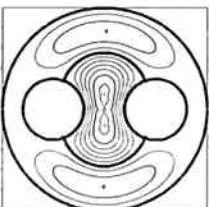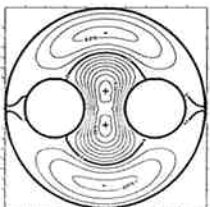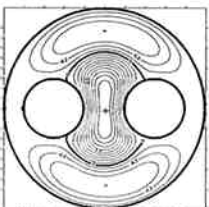
Table 6. The former five modes for a circle domain with two equal holes by using the present method, BEM and FEM.

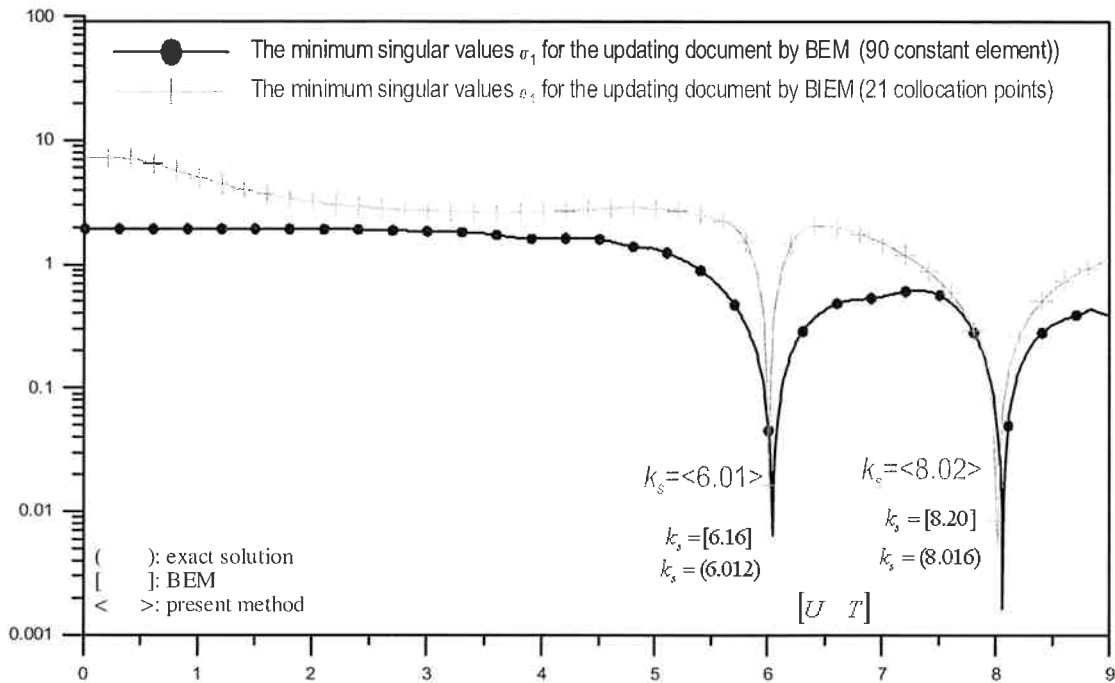| Mode	Present method ($M = 10$)	BEM[10]	FEM[10]
1 Symmetric with respect to x-axis	 $k = 4.53$	 $k = 4.50$	 $k = 4.45$
2 Antisymmetric with respect to x-axis	 $k = 4.53$	 $k = 4.50$	 $k = 4.45$
3 Symmetric with respect to x-axis	 $k = 6.4$	 $k = 6.37$	 $k = 6.27$
4 Antisymmetric with respect to x-axis	 $k = 6.4$	 $k = 6.37$	 $k = 6.27$
5 Symmetric with respect to x-axis	 $k = 7.1$	 $k = 7.16$	 $k = 6.93$

24   *J. T. Chen, C. T. Chen & I. L. Chen*

Fig. 11. Detection of spurious eigenvalues by using SVD updating document in the present method and BEM.

Table 7. The former five eigenvalues for a multiply-connected problem with two unequal holes by using different approaches.

Method	k_i				
	k_1	k_2	k_3	k_4	k_5
Burton & Miller method	4.82	4.82	6.72	6.72	7.82
Direct BEM + SVD Updating	4.81	4.81	6.73	6.73	7.81
Null-field BEM + SVD Updating	4.81	4.81	6.73	6.73	7.82
Fictitious BEM + SVD Updating	4.80	4.80	6.72	6.72	7.79
Direct BEM + CHIEF method	4.81	4.81	6.73	6.73	7.82
Null-field BEM + CHIEF method	4.83	4.83	6.74	6.74	7.84
Fictitious BEM + CHIEF method	4.77	4.77	6.68	6.68	7.88
FEM	4.79	4.80	6.62	6.63	7.80
Present method	4.85	4.85	6.77	6.77	7.91

6. Conclusions

For the eigenproblems with circular boundaries, we have proposed a special BIEM by using degenerate kernels, null-field integral equation and Fourier series in companion with adaptive observer systems. This method is a semi-analytical approach since only truncation error
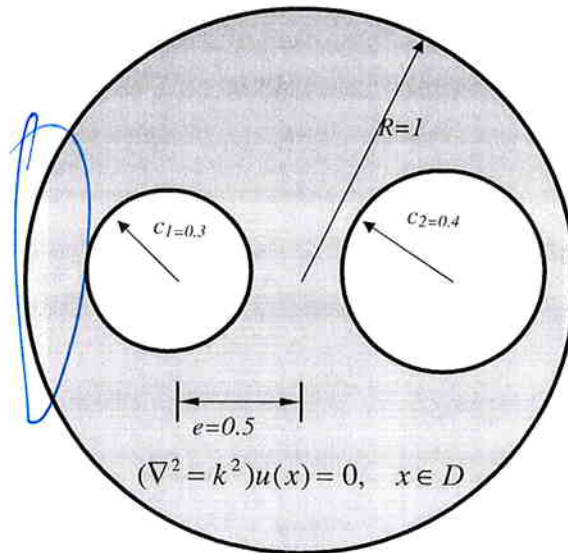
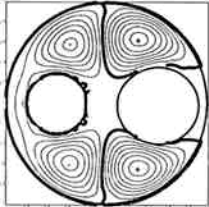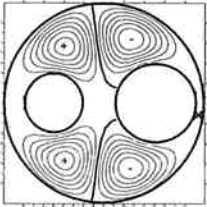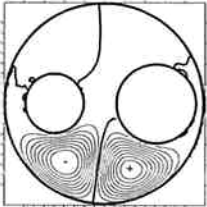Fig. 12. Two unequal circular holes in a circular domain.
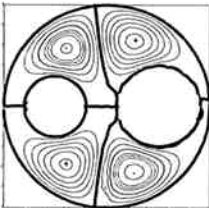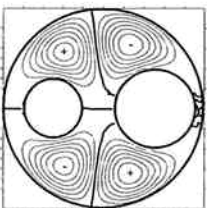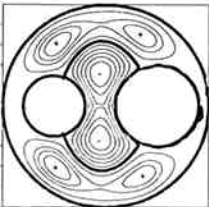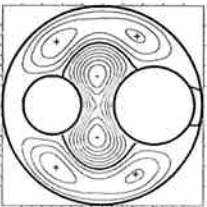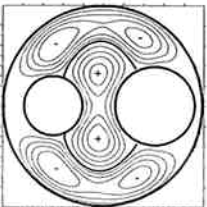
in the Fourier series is involved. The method shows great generality and versatility for the problems with multiple circular holes of arbitrary radii and positions. Also, the occurrence of spurious eigenvalue was examined and filtered by using SVD updating technique. Numerical results agree very well with those of the BEM and FEM. By using the same number of degree

Table 8. The former five modes for a circle domain with two unequal holes by using the present method, BEM and FEM.

Mode	Present method ($M = 10$)	BEM[15]	FEM[15]
1 Symmetric with respect to x-axis			
	$k = 4.85$	$k = 4.82$	$k = 4.80$
2 Antisymmetric with respect to x-axis			
	$k = 4.85$	$k = 4.82$	$k = 4.80$

26   *J. T. Chen, C. T. Chen & I. L. Chen*

Table 8. (*Continued*)

Mode	Present method ($M = 10$)	BEM[15]	FEM[15]
3 Symmetric with respect to x-axis	$k = 6.77$	$k = 6.72$	$k = 6.62$
4 Antisymmetric with respect to x-axis	$k = 6.77$	$k = 6.72$	$k = 6.63$
5 Symmetric with respect to x-axis	$k = 7.91$	$k = 7.82$	$k = 7.80$

of freedom, the present approach yields better result than BEM. Since the circular geometry is well captured by using Fourier series and degenerate kernel.

References

1. J. T. Chen and S. R. Lin, On the rank-deficiency problems in boundary integral formulation using the Fredholm alternative theorem and singular value decomposition technique, *WCCM5* Keynote lecture, Vienna, 2002.
2. P. W. Partridge, C. A. Brebbia and L. C. Wrobel, *The Dual Reciprocity Boundary Element Method* (Computer Mechchanics Publication, Southampton, 1992).
3. N. Kamiya and E. Andoh, A note on multiple reciprocity integral formulation for Helmholtz equation, *Comm. Num. Meth. Engng.* **9** (1993) 9–13.
4. A. J. Nowak and C. A. Brebbia, The multiple reciprocity method — a new approach for transforming BEM domain integrals to the boundary, *Engng. Analysis Bound. Elem.* **6** (1989) 164–167.
5. A. J. Nowak and A. C. Neves (eds.), *Multiple Reciprocity Boundary Element Method* (Computer Mechanics Publication, Southampton, 1994).
6. N. Kamiya, E. Andoh and K. Nogae, A new complex-valued formulation and eigenvalue analysis of the Helmholtz equation by boundary element method, *Adv. Engng. Soft.* **26** (1996) 219–227.

7. J. T. Chen, C. X. Huang and F. C. Wong, Determination of spurious eigenvalues and multiplicities of true eigenvalues in the dual multiple reciprocity method using the singular value decomposition technique, *J. Sound Vib.* **230** (2000) 219–230.

8. G. H. Golub and C. F. Van Loan, *Matrix Computations*, 2nd edn (The Johns Hopkins University Press, Baltimore, 1989).

9. I. L. Chen, J. T. Chen and M. T. Liang, Analytical study and numerical experiments for radiation and scattering problems using the CHIEF method, *J. Sound Vib.* **248**(5) (2001) 809–828.

10. I. L. Chen, J. T. Chen, S. R. Kuo and M. T. Liang, A new method for true and spurious eigensolutions of arbitrary cavities using the CHEEF method, *J. Acou. Soc. Amer.* **109** (2001) 982–999.

11. G. R. G. Tai and R. P. Shaw, Helmholtz equation eigenvalues and eigenmodes for arbitrary domains, *J. Acoust. Soc. Am.* **56** (1974) 796–804.

12. M. Kitahara, *Boundary integral equation methods in eigenvalue problems of elastodynamics and thin plates* (Elsevier, Amsterdam, 1985).

13. J. T. Chen, J. H. Lin, S. R. Kuo and S. W. Chyuan, Boundary element analysis for the Helmholtz eigenvalue problems with a multiply connected domain, *Proc. R. Soc. Lond. A* **457** (2001) 2521–2546.

14. J. T. Chen, L. W. Liu and S. W. Chyuan, Acoustic eigenanalysis for multiply-connected problems using dual BEM, *Comm. Num. Meth. Engng.* **20** (2004) 419–440.

15. J. T. Chen, L. W. Liu and H. K. Hong, Spurious and true eigensolutions of Helmholtz BIEs and BEMs for a multiply connected problem, *Proc. R. Soc. Lond. A* **459** (2003) 1891–1924.

16. J. T. Chen, I. L. Chen and Y. T. Lee, Eigensolutions of multiply-connected membranes using the method of fundamental solution, *Eng. Analy. Boun. Elem.* **29** (2005) 166–174.

17. Y. T. Lee, *Free Vibration of Membrane and Plate Problems by Using Meshless Methods*, Master Thesis, Department of Harbor and River Engineering, National Taiwan Ocean University, 2004.

18. W. H. Lin, Guided Waves in a Circular Duct Containing an Assembly of Circular Cylinders, *J. Sound Vib.* **79** (1981) 463–477.

19. K. Nagaya and K. Poltorak, Method for solving eigenvalue problems of the Helmholtz equation with a circular outer and a number of eccentric circular inner boundaries, *J. Acoust. Soc. Am.* **85** (1989) 576–581.

20. S. L. Crouch and S. G. Mogilevskaya, On the use of Somigliana's formula and Fourier series for elasticity problems with circular boundaries, *Int. J. Numer. Methods Eng.* **58** (2003) 537–578.

21. S. G. Mogilevskaya and S. L. Crouch, A Galerkin boundary integral method for multiple circular elastic inclusions, *Int. J. Numer. Methods Eng.* **52** (2001) 1069–1106.

22. J. Wang, S. G. Mogilevskaya and S. L. Crouch, A numerical procedure for multiple circular holes and elastic inclusions in a finite domain with a circular boundary, *Computational Mechanics* **32** (2002) 250–258.

23. M. R. Barone and D. A. Caulk, Optimal arrangement of holes in a two-dimensional heat conductor by a special boundary integral method, *Int. J. Numer. Methods Eng.* **18** (1982) 675–685.

24. M. R. Barone and D. A. Caulk, Special boundary integral equations for approximate solution of Laplace's equation in two-dimensional regions with circular holes, *Q. J. Mech. Appl. Math.* **34** (1981) 265–286.

25. M. R. Barone and D. A. Caulk, Special boundary integral equations for approximate solution of potential problems in three-dimensional regions with slender cavities of circular cross-section, *IMA J. Appl. Math.* **35** (1985) 311–325.

26. M. R. Barone and D. A. Caulk, Analysis of liquid metal flow in die casting, *Int. J. Eng. Sci.* **38** (2000) 1279–1302.

27. D. A. Caulk, Analysis of steady heat conduction in regions with circular holes by a special boundary integral method, *IMA J. Appl. Math.* **30** (1983) 231–246.

28. D. A. Caulk, Steady heat conduction from an infinite row of holes in a half-space or a uniform slab, *Int. J. Heat Mass Transfer.* **26** (1983) 1509–1513.

29. D. A. Caulk, Analysis of elastic torsion in a bar with circular holes by a special boundary integral method, *J. Appl. Mech.* **50** (1983) 101–108.

30. M. D. Bird and C. R. Steele, Separated solution procedure for bending of circular plates with circular holes, *Appl. Mech. Rev.* **44** (1991) 27–35.

31. M. D. Bird and C. R. Steele, A solution procedure for Laplace's equation on multiply-connected circular domains, *J. Appl. Mech.* **59** (1992) 398–404.

32. G. Chen and J. Zhou, *Boundary Element Method* (Academic Press, San Diego, 1992).

33. J. T. Chen, J. H. Lin, S. R. Kuo and Y. P. Chiu, Analytical study and numerical experiments for degenerate scale problems in boundary element method using degenerate kernels and circulants, *Eng. anal. bound. Elem.* **25**(9) (2001) 819–828.

34. J. R. Hutchinson, *Analysis of Plates and Shells by Boundary Collocation, in Boundary Elements Analysis of Plates and Shells*, ed. D. E. Beskos (Springer-Verlag, 1991), pp. 314–368.

35. S. R. Kuo, W. Yeih and Y. C. Wu, Applications of the generalized singularvalue decomposition method on the eigenproblem using the incomplete boundary element formulation, *J. Sound Vib.* **235** (2000) 813–845.